J. Fluid Mech. (1966), *vol.* 24, *part* 2, *pp.* 225–253
Printed in Great Britain

Equilibrium turbulent boundary layers

By G. L. MELLOR AND D. M. GIBSON†
Department of Aerospace and Mechanical Sciences, Princeton University

(Received 29 June 1964 and in revised form 31 March 1965)

Empirical information is extracted from constant-pressure flows and, on this basis alone, the equations of motion are solved for flows where the pressure gradient parameter, $\beta = \delta^*(dp/dx)/\tau_0$, is held constant. The experimental defect profiles of Clauser and the near-separating profile of Stratford are predicted quite well.

The present work is an extension of the work of Clauser and Townsend in that a particular form for an effective or eddy viscosity is hypothesized. Here, however, a continuous, and analytically precise family of defect profiles are calculated for the entire range, $-0{\cdot}5 \leqslant \beta \leqslant \infty$. The solutions span the whole profile with the exception of the viscous sublayer.

A detailed consideration of the viscous sublayer and a comparative examination of various eddy viscosity hypotheses are included in a companion paper.

1. Introduction

A theoretically derived determination of basic turbulent transfer processes seems beyond our grasp. Despite this, it is still possible to gain considerable understanding of the behaviour of turbulent boundary layers which are influenced by main stream pressure variations.

If one considers the general case of arbitrary pressure distribution it is clear that the existing theories are, in fact, a combination of established theory, empiricism and analytical approximation. A modest goal of turbulent boundary-layer research is to increase that which is theoretical, reduce analytical approximation, and then describe the empirical ingredients in as simple terms as possible. Out of this one hopes to achieve a fuller understanding of turbulent boundary-layer behaviour.

Clauser (1954, 1956) has made an important contribution toward this goal. In 1954 he singled out for study a class of simple 'equilibrium' boundary-layer flows which, in 1956, he associated with a main-stream pressure distribution characterized by the parameter, $\beta = \delta^*(dp/dx)/\tau_0 = \text{const}$. He also determined that one could analyze the outer portion of the boundary layer by assuming an eddy (or effective) viscosity, $\nu_e = KU\delta^*$, where K was an absolute constant.

As noted by Clauser (1954), the existing, general (arbitrary pressure gradient) boundary-layer theories fail to give correct answers for the simple, equilibrium case. Originally it was, and still is, our aim to construct a general theory which would, at least, eliminate this inconsistency. However, we quickly

† Present address: General Dynamics, Fort Worth, Texas.

found that the work started by Clauser was far from complete and did not yet provide a base from which to construct a more complicated theory. The present paper is therefore wholly concerned with equilibrium boundary layers.

Townsend (1956, 1960, 1961) has extended the analysis of Clauser and Stratford in order to produce further useful results. The basic physical assumption in the present paper and Townsend's later work are nearly identical and some of his results are similar to ours. However, Townsend's work, like Clauser's, is largely exploratory. As a result, the problem has been attacked piecemeal, and a considerable amount of analytical approximation and assumption is involved.

Some features of the present work are that:

(*a*) An effective viscosity hypothesis, presumed to be independent of pressure gradient and valid in the entire defect layer, is hypothesized.

(*b*) A well-posed formulation (equations (14), (15) and (16)) is set forth.

(*c*) The range of existence of non-separating equilibrium flows is established as $-0{\cdot}5 \leqslant \beta \leqslant \infty$.

(*d*) The equations are numerically integrated with precision through the entire defect layer and in the entire range, $-0{\cdot}5 \leqslant \beta \leqslant \infty$.

(*e*) The result is obtained that (for the sake of present and future analytical convenience) the second-order dependence of the defect profiles on Reynolds number may be neglected; the small error thus incurred has been calculated.

(*f*) The calculated profiles show good agreement with the experimental profiles of Clauser. Significantly, we obtain good agreement with the incipient separation profiles of Stratford (1959*b*) where $\tau_0(x) \simeq 0$. In this regard, a purely formal result of the theory is that defect profiles should be presented in the alternative form, $(U-u)/u_p$, instead of $(U-u)/u_\tau$ for large β, particularly when $1/\beta \to 0$ (u_τ is the conventional 'friction velocity', u_p is a 'pressure velocity' and $u_p/u_\tau = \beta^{\frac{1}{2}}$).

In a companion paper (Mellor 1966; hereafter referred to as paper B), the effect of pressure gradients on the flow immediately adjacent to a wall will be investigated.

2. Notation and definitions

x, y = co-ordinates parallel and perpendicular to the wall;
u, v = mean velocity components in the x, y directions;
p, ρ = pressure and density;
ν = kinematic molecular viscosity;
U = free-stream velocity; $U' = dU/dx$;
τ = total (turbulent plus molecular) shear stress;
$\nu_e = (\tau/\rho)/(\partial u/\partial y)$, effective (turbulent plus molecular) viscosity;
τ_0 = wall shear stress;
δ = approximate value of y marking the outer edge of the boundary layer;

$$\delta^* = \int_0^\infty (1-u/U)\,dy, \text{ displacement thickness;}$$

$$\theta = \int_0^\infty (u/U)(1-u/U)\,dy, \text{ momentum thickness;}$$

$H = \delta^*/\theta$, shape factor;

$u_\tau = (\tau_0/\rho)^{\frac{1}{2}}$, friction velocity;

$\gamma = u_\tau/U$; $c_f = 2\tau_0/\rho U^2 = 2\gamma^2$;

$\Delta = \int_0^\infty [(U-u)/u_\tau]\,dy = \delta^*/\gamma$, defect displacement thickness;

$\eta = y/\Delta = \gamma(y/\delta^*)$;

$f' = \partial f/\partial\eta = (U-u)/u_\tau$, velocity defect;

$G = \int_0^\infty [(U-u)/u_\tau]^2\,dy/\Delta = \int_0^\infty f'^2\,d\eta$, defect shape factor;

$\Phi = \nu_e/U\delta^*$;

$u_p = [(\delta^*\,dp/dx)/\rho]^{\frac{1}{2}}$, pressure velocity;

$\lambda = u_p/U$;

$\xi = \eta\beta^{\frac{1}{2}} = \lambda(y/\delta^*)$;

$F' = \partial F/\partial\xi = (U-u)/u_\rho = f'/\beta^{\frac{1}{2}}$;

$\mathbf{R} = U\delta^*/\nu$, Reynolds number;

$\beta = (\delta^*\,dp/dx)/\tau_0 = (u_p/u_\tau)^2 = \lambda^2/\gamma^2$, equilibrium boundary-layer parameter;

κ, K, B = empirical constants. (In this paper, $\kappa = 0{\cdot}41$, $K = 0{\cdot}016$, $B = 4{\cdot}9$.);

m = exponent in equation (32), defined by equation (30).

For purposes of stipulating an effective viscosity hypothesis, the two principal portions of the boundary layer are the *wall layer* and the *defect layer*. A portion, common to both, is the *overlap layer*. In the present paper we shall primarily be concerned with the defect layer.

3. The 'law of the wall' and velocity defect profiles

As in Clauser's analysis,† the starting-point of the present analysis is the realization that a set of experimental data typically in the form u/U vs y/δ may be rescaled into a wall form, $u/u_\tau = u^+(yu_\tau/\nu)$, and a defect form, $(U-u)/u_\tau = f'(y/\delta)$. If this is done for data at various Reynolds numbers, it is found that the wall form (or 'law of the wall') is universally valid for small values of yu_τ/ν, while the defect form is (nearly) universally valid for large values of y/δ. All of this is illustrated in figure 1 for two values of the Reynolds numbers (and where the length scale Δ has been used in place of δ). The small mismatch of the wall profile and the defect profiles evident in figure 1 should be ignored for the present; it will be discussed in § 8.

The foregoing considerations were initially suggested by von Karman and Prandtl and are fully discussed by Millikan (1938), who also found that the further assumption of the existence of a velocity overlap layer, which is described equally well by both forms, leads directly to the important conclusion that, in the overlap layer, u^+ and f' must be logarithmic. In fact, for our purposes, the logarithmic portion of the 'law of the wall' may be written

$$\frac{u}{u_\tau} = \frac{1}{\kappa}\ln\frac{u_\tau y}{\nu} + B. \tag{1}$$

† (*Added in proof.*) Throughout the writing of this paper we have unfortunately overlooked the work of Rotta (1950) who anticipated the value of defect and wall profiles and their inter-relationship.

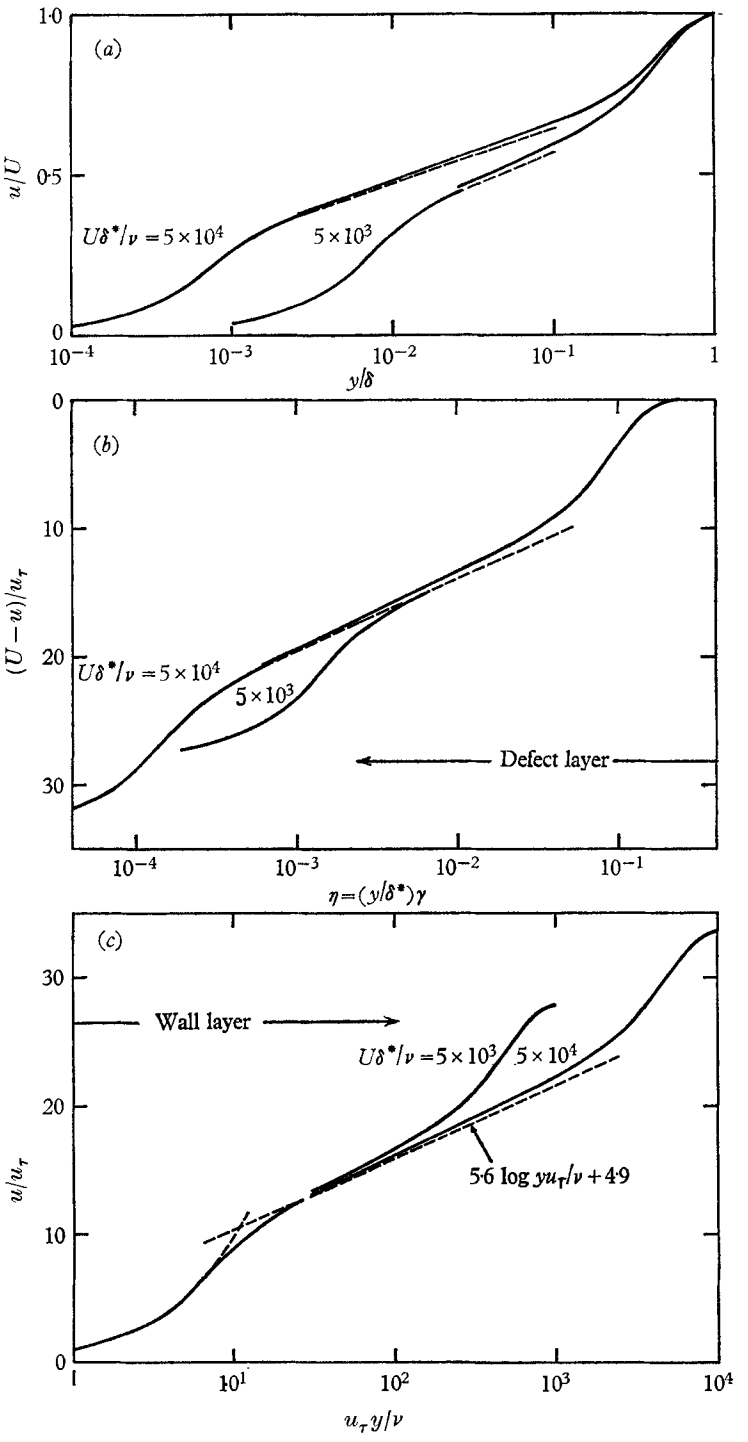

FIGURE 1. Illustration of the method of plotting velocity profiles (*a*), in the defect form (*b*), and the wall form (*c*). (The illustrative defect profile is taken from calculations when $\beta = 1$.)

The von Karman constant κ will be taken as 0·41, and $B = 4{\cdot}9$. Although there is some disagreement on the precise values of these constants, equation (1) is now believed to correlate data independently of the governing boundary conditions; that is, it is valid for pipes, channels, and boundary layers with or without pressure gradients. This last hypothesis was apparently established experimentally by Ludwig & Tillman (1950). We accept it tentatively, but will later find that it is subject to qualification.

The logarithmic form depends on the fact that $\tau \simeq \tau_0$ in a portion of the wall layer extending beyond the viscous sublayer. On the other hand, the defect layers must be influenced by the inertial and pressure gradient terms in the equations of motion and, through these equations, by the governing boundary conditions. In the present paper we are concerned with the boundary-layer problem, and it was Clauser's aim and it is the primary purpose of the present paper to predict the effect of pressure gradients on boundary-layer defect profiles.

It was Clauser's intuition that led him to attack the rather special class of pressure gradient where plots of $(U-u)/u_\tau$ vs y/δ are invariant at succeeding intervals of the streamwise co-ordinate. These 'equilibrium layers' which we now associate with constant values of β are, in some respects, analogous to the Falkner–Skan laminar boundary layers.

Although δ is a convenient length scale for the comparison of data, a more meaningful length scale is, as noted by Clauser,

$$\Delta \equiv \int_0^\infty \frac{U-u}{u_\tau}\,dy = \frac{\delta^*}{\gamma}, \tag{2}$$

where $\gamma = (\frac{1}{2}c_f)^{\frac{1}{2}}$ is a repeatedly useful notation.

An appropriate defect shape factor is

$$G \equiv \frac{1}{\Delta}\int_0^\infty \left(\frac{U-u}{u_\tau}\right)^2 dy, \tag{3}$$

and is related to the conventional shape factor, H, according to the relation

$$H^{-1} = \frac{1}{\delta^*}\int_0^\infty \frac{u}{U}\left(1-\frac{u}{U}\right) dy = 1-\gamma G. \tag{4}$$

It is instructive to note that, while G is a constant (or, as we will see later, nearly constant) for a given equilibrium layer, H depends strongly on γ.

4. The governing equations

Since we wish to integrate the time-averaged equations of motion, we shall adopt the Boussinesq definition of an 'effective viscosity' ν_e, such that

$$\tau/\rho \equiv \nu_e(\partial u/\partial y), \tag{5}$$

where we take τ to be the total stress which includes the molecular shear stress $\nu(\partial u/\partial y)$ as well as the Reynolds stress $-\overline{u'v'}$. Alternatively, we have $\nu_e = \nu_t + \nu$, where ν_t is the turbulent or eddy viscosity. In the light of the work of

Clauser (1954, 1956), Townsend (1956, 1960, 1961) and Stratford (1959*a*, *b*) on boundary-layer flows, it seems possible to make a reasonable assumption concerning ν_e which is not explicitly dependent on the pressure gradient. We shall consider such an assumption below.

The equations of motion for the mean velocities may now be written

$$u\frac{\partial u}{\partial x}+v\frac{\partial u}{\partial y}=U\frac{dU}{dx}+\frac{\partial}{\partial y}\left(\nu_e\frac{\partial u}{\partial y}\right), \tag{6}$$

$$\frac{\partial u}{\partial x}+\frac{\partial v}{\partial y}=0, \tag{7}$$

together with the boundary conditions

$$\lim_{y\to\infty}\int_0^y [U(x)-u(y',x)]\,dy' = U(x)\,\delta^*(x), \tag{8a}$$

$$v(0,x)=0, \tag{8b}$$

$$\lim_{y\to 0}\nu_e(y,x)\frac{\partial u(x,y)}{\partial y}=\tau_0(x). \tag{8c}$$

Equation (8*a*) is a stronger outer boundary condition than usually encountered in the literature. It not only requires that $u\to U$ as $y\to\infty$, but also requires that the displacement thickness (and the momentum thickness) be finite. This removes a lack of uniqueness of the type encountered by Hartree (1937) in his solution for laminar boundary layers.

Equation (8*c*) replaces the usual boundary condition $u(0,x)=0$ in the case of laminar boundary layers, and states merely that the shear stress must tend to the wall shear stress as $y\to 0$.

The effective viscosity assumption

We now wish to specify an effective viscosity hypothesis valid throughout the entire defect layer. In the present paper the discussion will be historically based, while in a companion paper (Mellor 1966, hereafter referred to as paper B) we shall attempt a more formal and complete discussion of the present hypothesis and other hypotheses encountered in the literature.

In the outer (approximately 80 %) part of a turbulent boundary layer it was Clauser's discovery that ν_e might be considered constant with respect to y. Any further refinement, such as allowing ν_e to approach ν for large y, presumably would not affect the calculated mean-velocity profiles appreciably. The important point is to determine the correct quantities on which to scale ν_e. For high Reynolds numbers, ν_e should be independent of viscosity (as is shown experimentally in the case of wakes and jets) in the outer layer, and it should be scaled on some dimension of the layer size and on some average (since ν_e is to be considered constant) of the velocity defect $U-u$. Since $U\delta^* \equiv \int_0^\infty (U-u)\,dy$ Clauser's stipulation that

$$\nu_e = KU\delta^* \quad \text{in the outer layer} \tag{9}$$

is not unreasonable. Here K, which is of the form of an inverse, turbulent Reynolds number, will be determined empirically in § 6. Including the values $\kappa = 0{\cdot}41$ and $B = 4{\cdot}9$ in equation (1), this raises to three the total number of empirical values required in the present analysis.

For the overlap layer, we shall assume the validity of Prandtl's mixing length theory:

$$\nu_e = \kappa^2 y^2 \left|\partial u/\partial y\right| \quad \text{in the overlap layer.} \tag{10}$$

Prandtl justified equation (10) on the basis of a physical argument which is now well known. Assuming $\tau(y) = \tau_0$, one directly obtains the logarithmic behaviour characterized by equation (1). A consequence of the present paper is that equation (10) appears to be valid even where $\tau(y) \gg \tau_0$.

Equations (9) and (10) can now be considered a single, continuous function (see equation (16)) if we define the dividing point between the overlap and the outer layer as the (smaller) value of y where $\kappa^2 y^2 \left|\partial u/\partial y\right| = KU\delta^*$.

A possible alternative is $\nu_e = l^2 \left|\partial u/\partial y\right|$, where the 'mixing length' $l = \kappa y$ near the wall. Then, in the outer portion, we could take $l = K'\delta$. It is our opinion that this alternative hypothesis probably would not yield results significantly different from the results based on equation (9). Note that if, as before, we take ν_e to be constant in the outer layer and, consistent with this, take $\partial u/\partial y$ as a constant, characteristic of the outer profile, then it is a simple step to show that $K \simeq 2K'^2$.

We should also like to mention the assumption adopted by Clauser (1956)† for the overlap layer. It may be written:

$$\nu_e = \kappa u_\tau y \quad \text{in the overlap layer.} \tag{10'}$$

Because of its simplicity, equation (10) was also adopted as the basis of some earlier work of the writers (Gibson & Mellor 1962).

We now find that equations (10) and (10′) yield nearly identical results as long as β is small. In fact, if $\tau = \tau_0$ in the overlap layer, the identity between equation (10) and equation (10′) may be easily established. However, the failure of equation (10′) for large β is clear in the limiting case $\beta = \infty$, or, equivalently, $u_\tau = 0$. We then obtain the unacceptable result $\nu_e = 0$.

The equation for $(U-u)/u_\tau$

It seems proper to seek defect solutions directly in the form

$$(U-u)/u_\tau = f'(\eta), \tag{11}$$

† Clauser (1956) never actually computed profiles in the overlap layer but assumed that they were logarithmic (or, equivalently, that $\tau \simeq \tau_0$) where $\nu_e = \kappa u_\tau y$. This latter relation was used only to determine a matching point, $y = KU\delta^*/\kappa u_\tau$, to graphically match the assumed, logarithmic, overlap layer to the outer layer computed with $\nu_e = KU\delta^*$. The matching procedure was awkward, and he only applied it to the case $\beta = 0$. We have found that the procedure would fail if applied to cases of, say, $\beta = 2$ and larger, since the the profiles are then no longer logarithmic at $y = KU\delta^*/\kappa u_\tau$.

Townsend (1956, 1960, 1961) did not independently define a matching point between the overlap and outer layer. This gave him a 'free' parameter with which to force a smooth match between two functions which were solutions of different approximate forms of the equations of motion.

so that
$$u = U(1-\gamma f'), \tag{11a}$$
$$\partial u/\partial x = U'(1-\gamma f') - U\gamma' f' + U\gamma(\Delta'/\Delta)\eta f'', \tag{11b}$$
$$\partial u/\partial y = -\gamma U f''/\Delta. \tag{11c}$$

And from equation (7), using the fact that $v(0) = 0$, we have

$$v = -\int_0 \frac{\partial u}{\partial x}\,dy = -U'\Delta(\eta-\gamma f) + U\Delta\gamma' f - U\gamma\Delta'(\eta f' - f). \tag{11d}$$

The stream-function f is defined so that $f(0) = 0$. The primes on f denote differentiation with respect to η, and primes on U, Δ and γ denote differentiation with respect to x.

If the above equations are inserted into equation (6) and if we set $\Phi = \nu_e/U\delta^*$, we obtain, after rearrangement,

$$\frac{1}{\beta}(\Phi f'')' - \left(\frac{\Delta' U}{\Delta U'}+1\right)(\eta f'' - \gamma f f'') + \frac{U\gamma'}{U'\gamma}(f' - \gamma f'^2 + \gamma f f'') + 2f' - \gamma f'^2 = 0, \tag{12}$$

where the important pressure-gradient parameter $\beta = -\delta^* U'/\gamma^2 U$ formally makes its first appearance.

Now, anticipating the result obtained for the parameter γ in § 8 (equation (26)) we find that

$$\frac{\gamma' U}{\gamma U'} = -\frac{\gamma/\kappa}{1+\gamma/\kappa}\left(\frac{\Delta' U}{\Delta U'}+1\right). \tag{13a}$$

This term was neglected entirely by Clauser (1956) on the basis that γ is a slowly varying function of x. We find, however, that it contributes a term of the same order as some of the terms already present.

Now, the quantity $(\Delta' U/\Delta U' + 1)$ may be obtained by integrating equation (12) from $\eta = 0$ to ∞. With the help of integrals like

$$\int_0^\infty f'\,d\eta = -\int_0^\infty \eta f'\,d\eta = 1, \quad \int_0^\infty f'^2 d\eta = -\int_0^\infty f f''\,d\eta = G,$$

we obtain
$$\frac{\Delta' U}{\Delta U'} + 1 \equiv \frac{1}{m} + 1 = -\left(1+\frac{\gamma}{\kappa}\right)\frac{\beta^{-1} + 2 - \gamma G}{1 - \gamma G + \gamma^2 G \kappa^{-1}}, \tag{13b}$$

which is a form of the von Karman integral equation. The reason for defining m in this particular way will be made clear in §§ 5 and 9. Combining equations (12) and (13a, b), we have

$$(\Phi f'')' - \beta\left(\frac{1}{m}+1\right)\left[\eta f'' - \gamma f f'' + \frac{\gamma/\kappa}{1+\gamma/\kappa}(f' - \gamma f'^2 + \gamma f f'')\right] + \beta(2f' - \gamma f'^2) = 0. \tag{14}$$

Note that, although we have defined m for convenience, equation (14) contains only the parameters β and γ. In our present nomenclature the boundary conditions are

$$\lim_{\eta\to\infty} f(\eta) = 1, \tag{15a}$$
$$f(0) = 0, \tag{15b}$$
$$\lim_{\eta\to 0} \Phi(\eta) f''(\eta) = -1. \tag{15c}$$

The effective viscosity corresponding to equations (9) and (10) may be written

$$\left.\begin{aligned}\frac{\nu_e}{U\delta^*} \equiv \Phi(Z) = Z(\eta),\ \eta \leqslant e,\\ = K,\ \eta \geqslant e,\end{aligned}\right\} \tag{16}$$

where we have set $Z = \kappa^2\eta^2|f''|$. The quantity e, defining the edge of the overlap layer, is determined from the equation $Z(e) = K$. This latter equation will generally have two roots, so that we must specify e as being the smaller of the two.

The behaviour of Φ should, in reality, be such that $\Phi \sim 1/R$ or $\nu_e \sim \nu$ as $\eta \to 0$. However, in our subsequent calculations we shall apply equation (16) everywhere, and we shall see that $f' \sim -(1/\kappa)\ln\eta + \text{const.}$ as $\eta \to 0$. The problem of connecting this limiting form with the physically correct behaviour $u \to 0$ as $\eta \to 0$ will be discussed in § 8 and more thoroughly in paper B.

Except for the fact that we plan to solve equation (14) across the whole defect layer and to account for the parameter γ, equation (14) is somewhat similar to that obtained by Townsend. It is worth noting that Townsend (1956, 1960) did not explicitly adopt the length scale Δ, but instead ν/u_τ, and several variables associated with the defect profiles are cast directly in the form of Reynolds number. Conceptually, this is confusing since the essential feature of defect profiles are that they are (almost) independent of Reynolds number.

The transformation for large β

It is clear that as $\beta \to \infty$, and correspondingly $u_\tau \to 0$, values of f' at some fixed value of η will increase indefinitely. This trend was, of course, evident in our calculations and it was also evident that the approximate value of η marking the edge of the boundary layer decreased as β increased (such that, for all β, $\int_0^\infty f'\,d\eta = 1$). This led to the realization that computations for very large β, and in particular for $\beta = \infty$, could be made after effecting the following transformations:

$$\eta = \xi/\beta^{\frac{1}{2}}, \tag{17a}$$

$$f(\eta) = F(\xi) \quad \text{or} \quad f'(\eta) = \beta^{\frac{1}{2}}F'(\xi), \tag{17b}$$

$$\gamma = \lambda/\beta^{\frac{1}{2}}. \tag{17c}$$

Substitution of equations (17*a*, *b*, *c*) into equation (14) yields

$$(\Phi F'')' - \left(\frac{1}{m}+1\right)\left[\xi F'' - \lambda F F'' + \frac{\lambda/\kappa\beta^{\frac{1}{2}}}{1+\lambda/\kappa\beta^{\frac{1}{2}}}(F' - \lambda F'^2 + \lambda F F'')\right] + 2F' - \lambda F'^2 = 0. \tag{18}$$

The boundary conditions are

$$\lim_{\xi\to\infty} F(\xi) = 1, \tag{19a}$$

$$F(0) = 0, \tag{19b}$$

$$\lim_{\xi\to 0} \Phi(\xi)F''(\xi) = -\frac{1}{\beta}. \tag{19c}$$

The definition of Φ remains the same as in equation (16), except now

$$Z = Z(\xi) = -\kappa^2\xi^2F''.$$

Equation (19*c*) represents the non-dimensional shear stress at the wall, which vanishes as $\beta \to \infty$.

The transformation in equations (17 *a*, *b*, *c*) has an appealing physical interpretation. If we define a 'pressure velocity', $u_p \equiv [(\delta^* dp/dx)/\rho]^{\frac{1}{2}}$, then $\beta^{\frac{1}{2}} = u_p/u_\tau$ is the ratio of the pressure velocity to the 'friction velocity', and it is seen that

$$(U-u)/u_p = F'(\xi), \tag{20}$$

and that $\lambda = u_p/U$.

5. Range of possible equilibrium solutions

It is instructive to consider equation (14) for the case $\gamma = 0$ ($\mathbf{R} = \infty$) and in the outer region where $\Phi = K$. We then obtain

$$Kf_0''' + (1+2\beta)\eta f_0'' + 2\beta f_0' = 0. \tag{21}$$

Equation (21) is a linear, confluent hypergeometric equation, further details of which are discussed in Appendix A. In particular it is found that, for very large η, f_0' behaves like

$$f_0' \sim e^{-x} x^{-a}\left[1 + O\left(\frac{1}{x}\right)\right],$$

where $x = (2\beta+1)\eta^2/2K$ and $a = 1/2(2\beta+1)$. Solutions exist only when $(2\beta+1) \geqslant 0$, or in the range $-0{\cdot}5 \leqslant \beta \leqslant \infty$ (at $\beta = -0{\cdot}5$, $f_0' \sim e^{-\eta/K}$). For $\beta < 0{\cdot}5$, no solution exists which vanishes as $\eta \to \infty$. Note that the condition $\beta > 0$ corresponds to decelerating flows, and the condition $\beta < 0$ to accelerating flows.

If now one examines equation (14) when η is large, the term f'^2 may be neglected and $f \simeq 1$. The resulting equation is again in the form of a confluent hypergeometric equation, and we find now that solutions exist when $-2\beta(1+1/m) \geqslant 0$. From equation (13*b*) it will be seen that this is the same result as before if $\gamma = 0$. However, for $\gamma \neq 0$, the lower limit $\beta \geqslant -0{\cdot}5$ is replaced by the condition $m \geqslant -1$. This corresponds to a value of β slightly lower than $-0{\cdot}5$.

For simplicity, we shall refer to the range of possible solutions as $-0{\cdot}5 \leqslant \beta \leqslant \infty$, with the understanding that the lower limit needs to be amended slightly.

In all of this discussion the possibility of reverse flow is excluded; that is, $\tau_0 \geqslant 0$.

6. The calculated profiles

We first turn our attention to the constant-pressure case, $\beta = 0$. Tentatively we will set $\gamma = 0{\cdot}04$, which is a typical value. By comparison of the calculated profile with the data shown in figure 2, the value $K = 0{\cdot}016$ was chosen (which gave only slightly better agreement than the value $K = 0{\cdot}018$ used by Clauser), and this will hereafter be applied to all values of β.

When Clauser initiated his experimental inquiry into equilibrium boundary layers he first assumed that $f' = (U-u)/u_\tau$ was independent of Reynolds number, or equivalently, of γ. As is apparent from equation (14), this is not the

case. However, it is found that f' is only weakly dependent on γ; this suggests that solutions might be obtained in the form

$$f' = f'_0 + \gamma f'_1 + \ldots,$$

or

$$F' = F'_0 + \lambda F'_1 + \ldots.$$

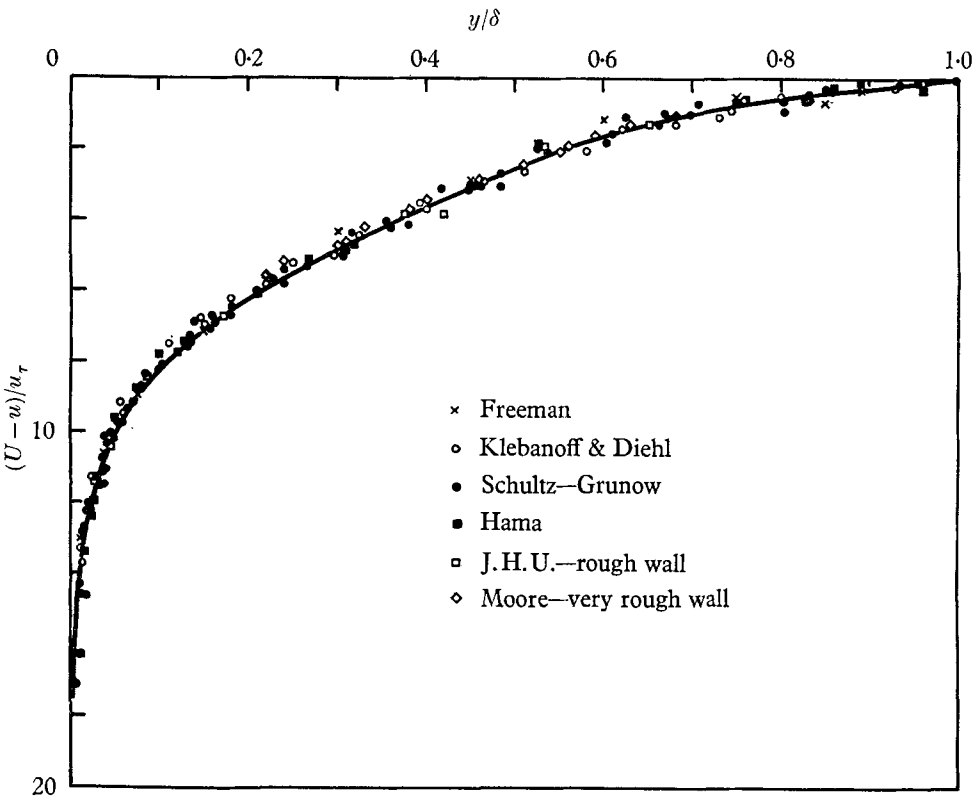

FIGURE 2. Equilibrium defect profiles for $\beta = 0$ (constant pressure). The data are from Clauser (1954). The solid line is calculated, and the constant $K = 0{\cdot}016$ is determined.

This approach is described in some detail in Appendix B. Numerical calculations yielded (on an IBM 7090; for details see Appendix C) the functions $f'_0(\eta), f'_1(\eta)$ or $F'_0(\xi), F'_1(\xi)$ for the complete range of β.

Then, in order to make some statement about the accuracy of the truncated series, we made computations directly from equation (14) or (18) (see Appendix C). In figure 3 we have abstracted a single result from each profile, namely the variation $\Delta f'$ or $\Delta F'$ with respect to γ or λ for vanishingly small values of η or ξ. The effect of γ or λ is most pronounced when η or ξ is small. The dashed lines represent the linear result from the two-term series expansion, where $\Delta f' = \gamma f'_1(0)$ or $\Delta F' = \lambda F'_1(0)$.

We have been able to obtain the function $\gamma(\beta, \mathbf{R})$ or $\lambda(\beta, \mathbf{R})$ in § 8. Therefore, for the present purpose we shall consider the lines of constant $\mathbf{R}$ drawn in figure 3 as iterative, consideration of which will be verified in § 8 (and subjected to slight modification in paper B).

Figure 3 indicates that the linearization $f' = f'_0 + \gamma f'_1$ or $F' = F'_0 + \lambda F'_1$ is fairly accurate, and we could proceed on this basis. However, in order that our final results be in the simplest possible form, we decided to present solutions directly from equations (14) or (18) for values of γ or λ when $\mathbf{R} = 10^5$. The reason behind this decision is that, according to figure 3, the maximum variation in the range

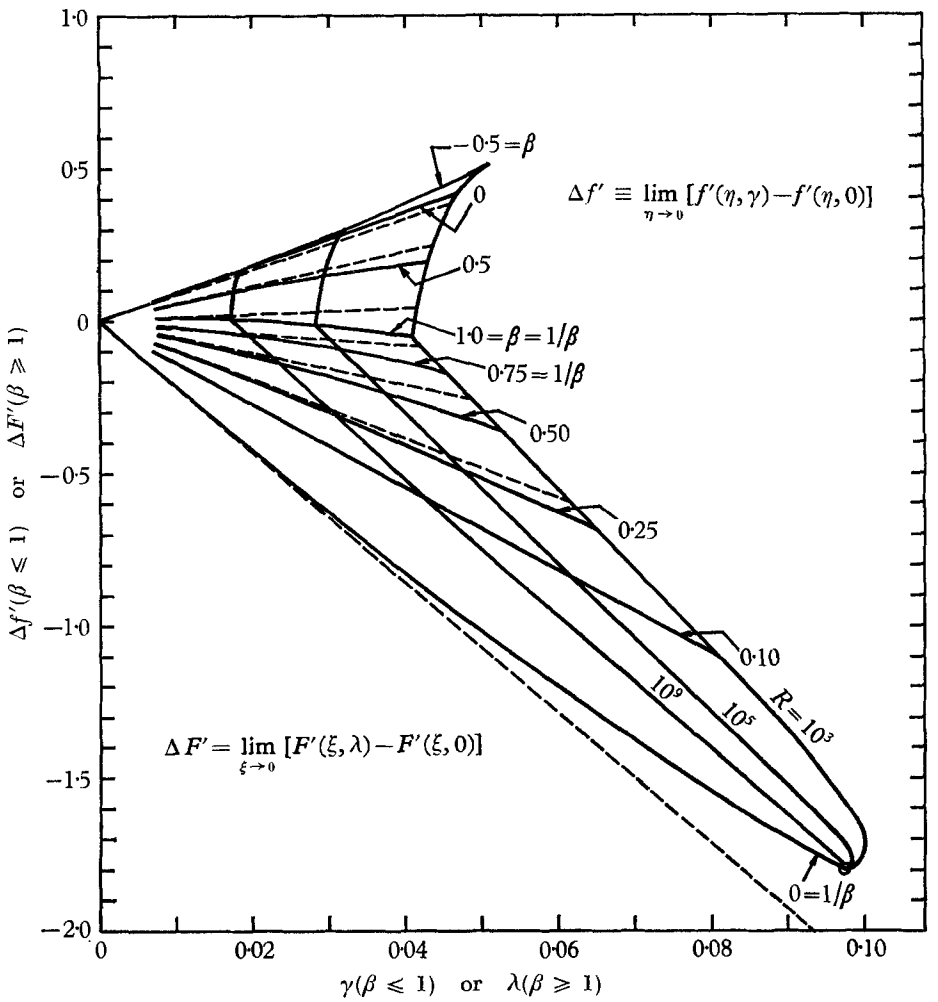

FIGURE 3. For small η, the variation of f' with respect to γ when $\beta \leqslant 1$; for small ξ, the variation of F' with respect to γ when $\beta \geqslant 1$.

$10^3 \leqslant \mathbf{R} \leqslant 10^9$ is less than 2 % of the main-stream velocity, and it is probable that the variation cannot be detected experimentally. For the data discussed below, this theoretical variation is much less than 2 %. Solutions for $\mathbf{R} = 10^5$ are therefore presented in table 1 and are plotted in figures 4 and 5.

By now it will have occurred to some readers that we had originally assumed $f' = f'(\eta)$ and have found that $f' = f'(\eta, \gamma)$. This means that equation (11*b*), and

therefore the following equations, should include the term $\gamma' \partial f'/\partial\gamma$. However, from the linearized solution we find that $\gamma' \partial f'/\partial\gamma = \gamma' f_1'$. It is then possible to reinsert this term in equation (11*b*), carry it through the analysis and assess its effect on the final solutions; we find that the error due to neglect of the term is less than 0·1 % and is therefore negligible. In this regard, we note that

β	-0.5	0·0	0·5	1·0	0·75	0·50	0·25	0·10	0·0	$1/\beta$
A	-2.54	-0.59	1·07	2·53	2·97	3·54	4·58	5·84	10·27	$A/\beta^{\frac{1}{2}}$
G	4·74	6·58	8·01	9·18	8·56	7·87	7·08	6·49	5·90	$G/\beta^{\frac{1}{2}}$
η	f'	f'	f'	$f'=F'$	F'	F'	F'	F'	F'	ξ
0·0001	19·91	21·86	23·53	24·98	22·71	20·05	16·65	13·79	10·12	0·0001
0·0002	18·22	20·17	21·83	23·29	21·25	18·85	15·80	13·24	10·05	0·0002
0·0005	15·99	17·93	19·60	21·04	19·30	17·25	14·67	12·52	9·93	0·0005
0·0010	14·31	16·24	17·90	19·33	17·82	16·04	13·80	11·96	9·78	0·0010
0·0020	12·63	14·55	16·19	17·61	16·32	14·80	12·91	11·37	9·58	0·0020
0·0050	10·44	12·32	13·91	15·29	14·29	13·12	11·66	10·51	9·17	0·0050
0·0100	8·81	10·64	12·16	13·46	12·68	11·77	10·65	9·75	8·72	0·0100
0·0200	7·23	8·96	10·37	11·54	10·97	10·30	9·48	8·83	8·08	0·0200
0·0300	6·34	7·99	9·30	10·36	9·90	9·36	8·71	8·20	7·60	0·0300
0·0400	5·73	7·31	8·49	9·38	9·06	8·65	8·11	7·69	7·20	0·0400
0·0500	5·27	6·72	7·70	8·35	8·19	7·95	7·59	7·26	6·85	0·0500
0·0600	4·87	6·16	6·92	7·32	7·29	7·20	7·01	6·82	6·53	0·0600
0·0700	4·49	5·61	6·14	6·29	6·38	6·43	6·41	6·33	6·18	0·0700
0·0800	4·14	5·08	5·38	5·31	5·50	5·66	5·77	5·80	5·79	0·0800
0·0900	3·82	4·57	4·66	4·40	4·65	4·90	5·13	5·26	5·36	0·0900
0·1000	3·52	4·09	3·99	3·57	3·87	4·18	4·50	4·71	4·91	0·1000
0·1200	2·99	3·22	2·81	2·22	2·53	2·89	3·31	3·62	3·98	0·1200
0·1400	2·53	2·48	1·87	1·26	1·53	1·86	2·28	2·63	3·05	0·1400
0·1600	2·14	1·85	1·18	0·66	0·85	1·11	1·48	1·80	2·21	0·1600
0·1800	1·81	1·35	0·70	0·31	0·44	0·62	0·90	1·16	1·50	0·1800
0·2000	1·52	0·96	0·39	0·14	0·20	0·32	0·51	0·70	0·95	0·2000
0·2500	0·99	0·36	0·07	0·01	0·02	0·04	0·09	0·15	0·22	0·2500
0·3000	0·63	0·11	0·01	0·00	0·00	0·00	0·01	0·20	0·03	0·3000
0·3500	0·40	0·03	0·00	—	—	—	0·00	0·00	0·00	0·3500
0·4000	0·25	0·01	—	—	—	—	—	—	—	0·4000
0·4500	0·16	0·00	—	—	—	—	—	—	—	—
0·5000	0·09	—	—	—	—	—	—	—	—	—
0·6000	0·03	—	—	—	—	—	—	—	—	—
0·7000	0·01	—	—	—	—	—	—	—	—	—
0·8000	0·00	—	—	—	—	—	—	—	—	—

(Note. The computations were accurate to the third decimal place. Since this is hardly significant physically the tabulated numbers have been rounded to the second decimal place.)

TABLE 1. $f'(\eta)$ when $-0.5 \leqslant \beta \leqslant 1.0$ and $F'(\xi)$ when $1.0 \leqslant \beta \leqslant \infty$

Townsend (1956) has singled out the two cases where $\gamma(x) = \text{const.}$ or where $\gamma' \partial f'/\partial\gamma = 0$. The first instance occurs when $m = -1$ (see equations (26) and (31)) and the second when $\beta = \infty$ (or when $\gamma = 0$). These cases represent equilibrium profiles in a theoretically exact sense. However, we have determined that the distinction is quantitatively meaningless and deserves no special consideration.

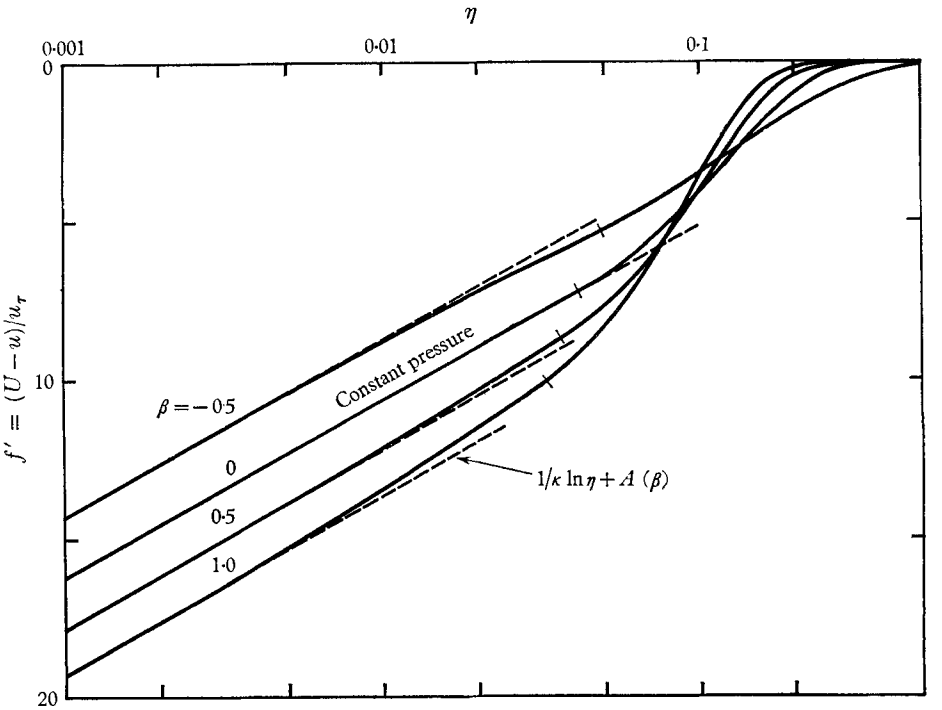

FIGURE 4. Calculated defect profiles for small β. The dividing point between overlap and outer layer is indicated by a small cross-line.

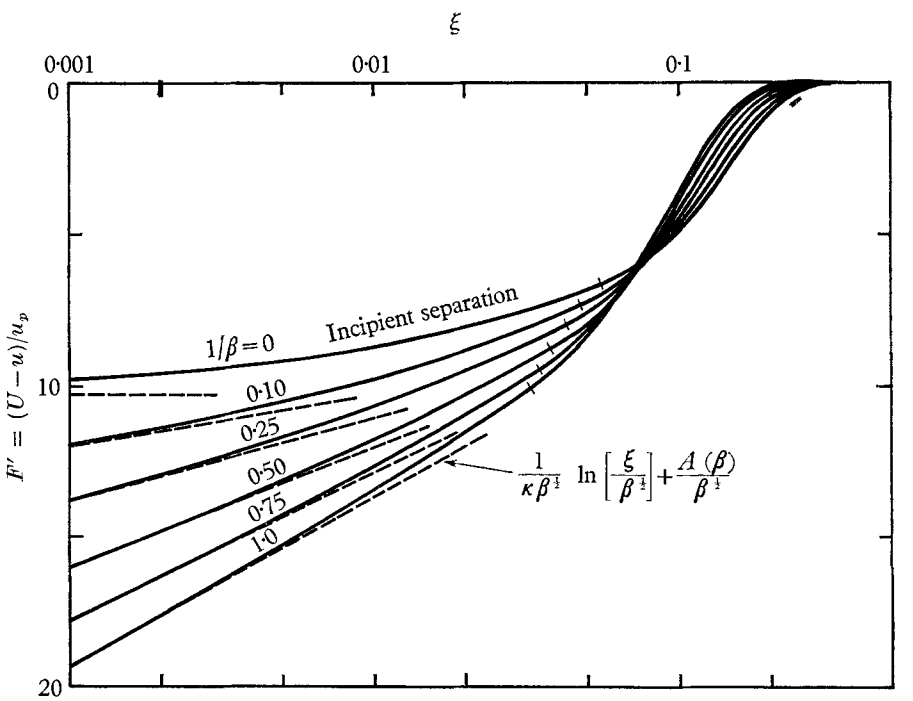

FIGURE 5. Calculated defect profiles for large β. The dividing point between overlap and outer layer is indicated by a small cross-line.

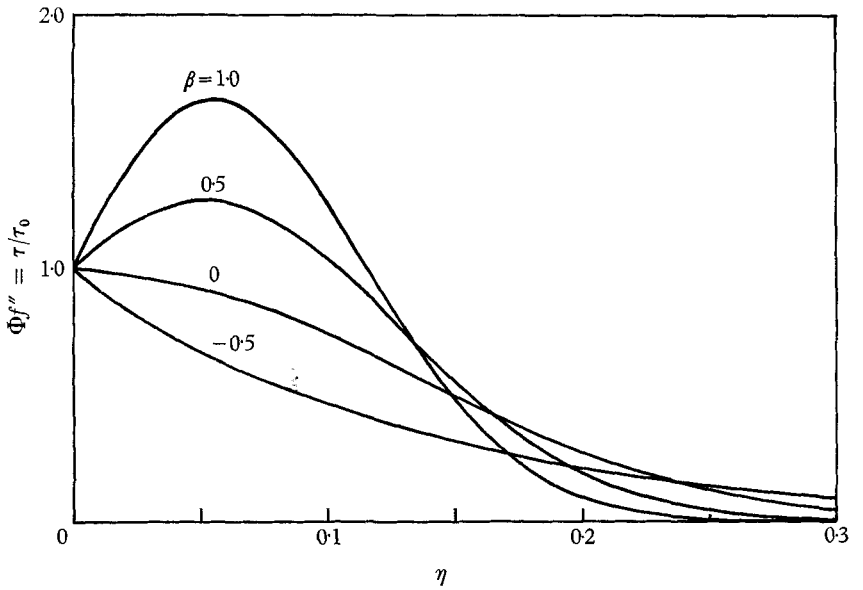

FIGURE 6. Variation of total stress for small β.

Shear-stress distribution

An interesting by-product of our calculation is the shear-stress distribution presented in the form $\tau/\tau_0 = -\Phi f''$ (figure 6) and in the form $\tau/\rho u_p^2 = -\Phi F''$ (figure 7).

7. Comparison of theory and data

Clauser's data

In figure 8, theory and data are compared for the non-zero pressure-gradient data of Clauser (1954). The appropriate values of β were determined by an examination of Clauser's data† for $U(x)$ and $\delta^*(x)$. First of all we learned that, experimentally, β was not precisely constant.

In the case of pressure distribution 1, β was nearly constant at a value slightly less than 1·80 in the range 83 in. $< x <$ 323 in., but then increased to around 2·25 in the much smaller range (relative to δ^*) 323 in. $< x <$ 387 in. The value $\beta = 1{\cdot}8$ seemed to be the more accurate choice instead of the value 2·0 previously quoted by Clauser.

In the case of pressure distribution 2, we found that, experimentally, β increased almost linearly from a value of 6 at $x = 100$ in. to a value of 13 at $x = 320$ in. in the range 152 in. $\leqslant x \leqslant$ 230 in., the value $\beta = 8$ seemed correct, but this is not an altogether clear choice. Nevertheless, any of the theoretical curves in the range $7 \leqslant \beta \leqslant 9$ would not differ greatly from the data.

It should be noted that Coles (1956) has discovered that Clauser's data do not satisfy the two-dimensional momentum-integral equation very well; this is presumably due to the presence of secondary flows. Strangely enough, this

† The authors wish to thank Prof. Clauser for making the tabulated data available to us.

experimental inconsistency is even more pronounced with the data for $\beta = 1{\cdot}8$ than it is with the data for $\beta = 8{\cdot}0$, and it may serve to explain why discrepancies between theory and data for small y are evident when $\beta = 1{\cdot}8$.

Perhaps we are splitting hairs; the overall conclusion must be that agreement between theory and data is remarkably good.

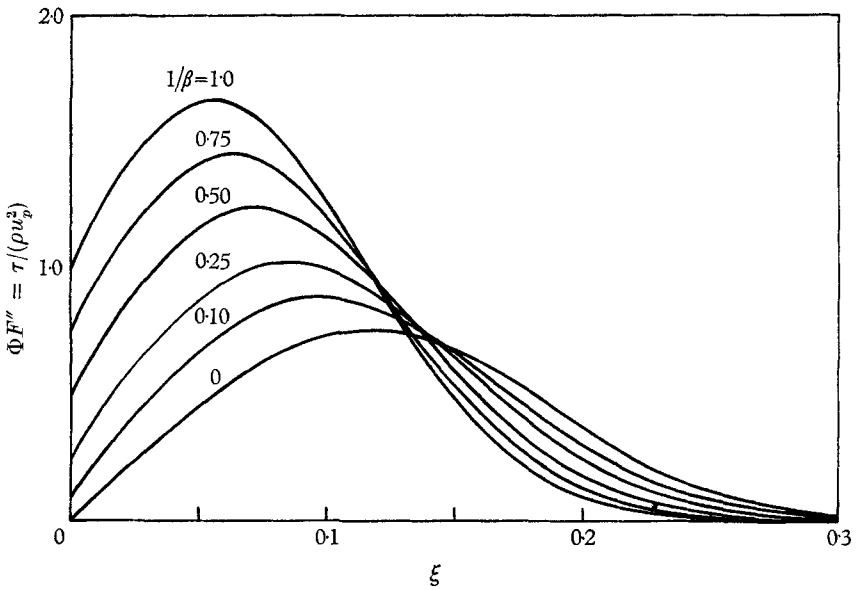

FIGURE 7. Variation of total stress for large β.

Stratford's data for near-separating flow

For not too large a value of β, or not too small a value of $\mathbf{R}$, $f'(\eta)$ or $F'(\xi)$ are logarithmic for large enough η or ξ, so that an overlap is established with the logarithmic position of the law of the wall. The law of the wall, in turn, establishes the connexion with the true boundary condition $u = 0$ at $y = 0$.

However, for the case $\beta = \infty$, a logarithmic portion does not exist at all. In fact, it may be seen by comparison with the values listed in table 1 that, for small enough ξ,

$$(U-u)/u_p \equiv F' = 10{\cdot}27 - 15{\cdot}6\xi^{\frac{1}{2}}. \tag{22}$$

We must now make an assumption which replaces the usual role of the law of the wall. We will assume that the increase of u from its value zero, through the viscous sublayer to the region where the profile is presumably described by equation (22), is negligible. Assuming $\tau = (dp/dx)y$ near the wall and equation (10), Stratford (1959*a*) has already shown that

$$u = \frac{2}{\kappa}\left(\frac{1}{\rho}\frac{dp}{dx}\right)^{\frac{1}{2}} y^{\frac{1}{2}} + C\left(\frac{\nu}{\rho}\frac{dp}{dx}\right)^{\frac{1}{3}}, \tag{23}$$

where the second term on the right-hand side (C is a constant) may be considered a slip velocity which is proportional to $u_p/\mathbf{R}^{\frac{1}{3}}$. Our assumption is therefore that

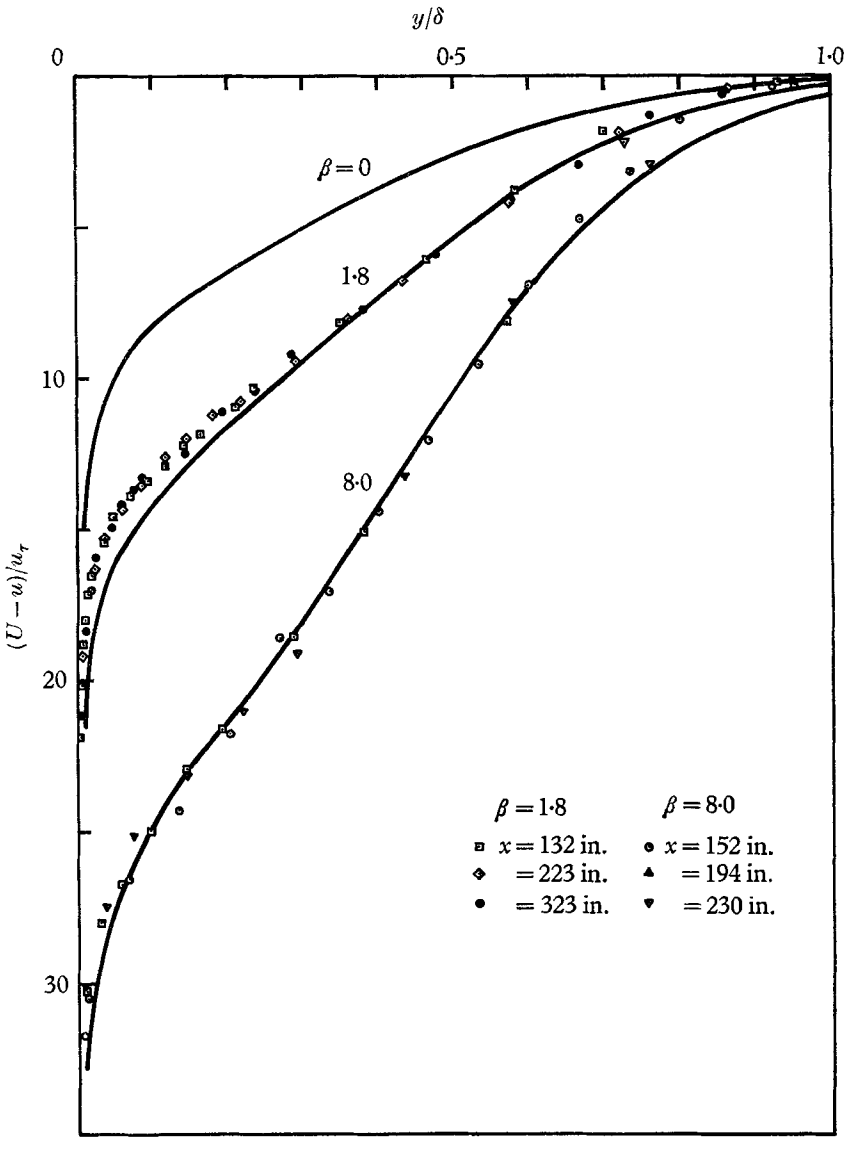

FIGURE 8. Equilibrium defect profiles for $\beta \geqslant 0$. The data are from Clauser (1954). The solid lines are calculated.

the constant of proportionality is small in comparison with typical experimental values of $\mathbf{R}^{\frac{1}{3}}$. Nevertheless, we regard this assumption as a temporary expediency which will be re-examined in paper B.

If in equation (22) we now set $u = 0$ at $\xi = 0$, we obtain $u_p/U = \lambda = 1/10{\cdot}27$, or

$$\lambda^2 \equiv -U'\delta^*/U = 0{\cdot}00948. \tag{24}$$

Stratford (1959*b*) has obtained a remarkable set of data. By trial-and-error adjustment of the pressure distribution he obtained velocity profiles at successive streamwise stations, so that, near the wall, the condition $u \sim y^{\frac{1}{2}}$ was approxi-

mately satisfied. This, then, should conform to the condition $\tau_0 = 0$ or $\beta = \infty$. From his data† for $U(x)$ and $\delta^*(x)$, our best estimate of $-U'\delta^*/U$ is 0·010, in good agreement with the theoretical results in equation (24).

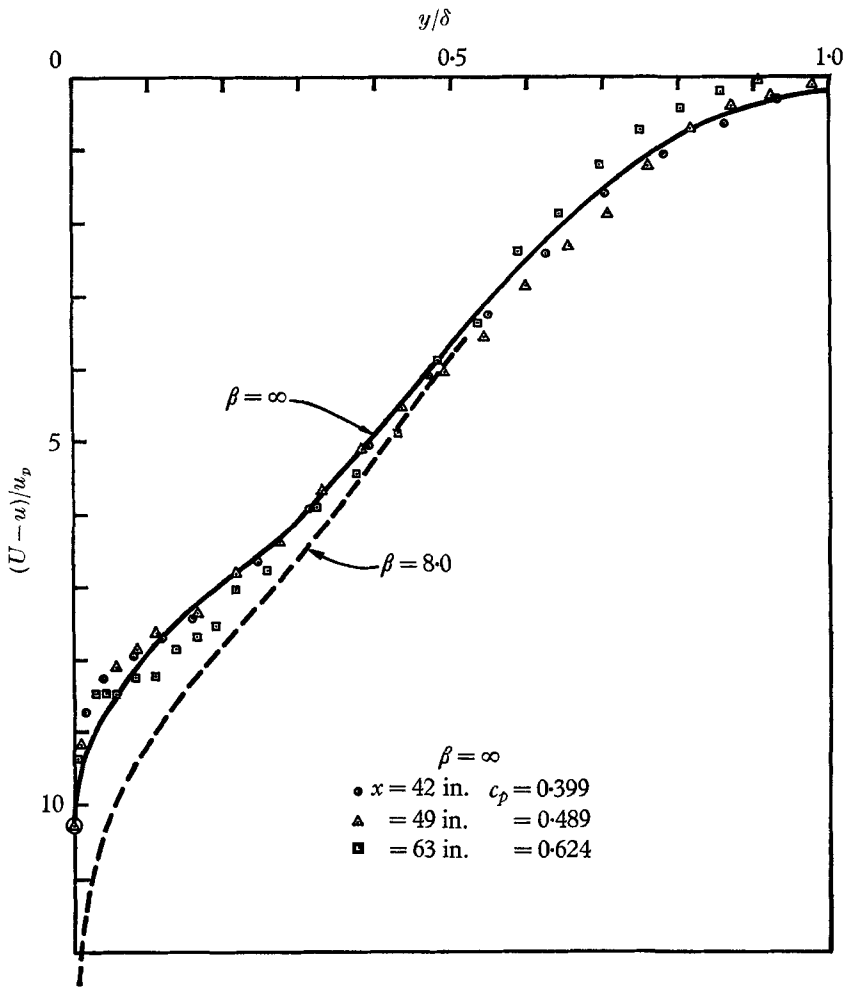

FIGURE 9. Equilibrium defect profile for $\beta = \infty$. The data are from Stratford (1959*b*) and are compared with the calculated solid line. In the range $0 \leqslant y/\delta \leqslant 0{\cdot}30$, $u \sim y^{\frac{1}{2}}$. The dashed line for $\beta = 8$ is from figure 8.

In figure 9, Stratford's profiles are compared with the theory. It should be noted that in this plot the point at $y = 0$ (where $u = 0$) must be considered a significant data point. We have also included, for comparison, a profile from figure 8 which has been rescaled according to the relation

$$(U-u)/u_p = (U-u)/u_\tau \beta^{\frac{1}{2}}.$$

If Stratford's data were not available, the case $\beta = \infty$ might have been considered a rather interesting but, perhaps, idealized limiting case of the theory.

† We wish to thank Dr Stratford for making the tabulated data available to us.

However, its experimental existence is gratifying and represents a significant plank in the overall theoretical structure. Conversely, the theory establishes the rightful role of this set of data as one member of a large continuous family in the range $-0{\cdot}5 \leqslant \beta \leqslant \infty$.

Consideration of Stratford's data will be slightly refined in paper B.

8. The skin-friction coefficient and the defect shape factor

For small β, it may be seen in figure 4 that

$$(U-u)/u_\tau = f'(\eta) = -\kappa^{-1}\ln\eta + A(\beta), \tag{25a}$$

where the defect constant A is given by

$$A(\beta) = \lim_{\eta\to 0}[f'(\eta,\beta)+\kappa^{-1}\ln\eta]. \tag{25b}$$

Values of A are tabulated in table 1. If we now assume the existence of a velocity overlap where u is described equally well by equations (1) or (25a), these equations may be added to give the skin-friction equation

$$\frac{1}{\gamma} = \left(\frac{2}{c_f}\right)^{\frac{1}{2}} = \kappa^{-1}\ln\frac{U\delta^*}{\nu} + A + B. \tag{26}$$

For large β, we note that equations (25a, b) may be conveniently written

$$\frac{U-u}{u_p} = -\frac{1}{\kappa\beta^{\frac{1}{2}}}\ln\frac{\xi}{\beta^{\frac{1}{2}}} + \frac{A(\beta)}{\beta^{\frac{1}{2}}}, \tag{25a'}$$

where

$$\frac{A(\beta)}{\beta^{\frac{1}{2}}} = \lim_{\xi\to\infty}\left[F'(\xi,\beta)+\frac{1}{\kappa\beta^{\frac{1}{2}}}\ln\frac{\xi}{\beta^{\frac{1}{2}}}\right]. \tag{25b'}$$

For large β equation (26) may also be written

$$\frac{1}{\lambda} = \frac{1}{\kappa\beta^{\frac{1}{2}}}\ln\frac{U\delta^*}{\nu} + \frac{A}{\beta^{\frac{1}{2}}} + \frac{B}{\beta^{\frac{1}{2}}}. \tag{26'}$$

When $1/\beta = 0$, we have $1/\lambda = A/\beta^{\frac{1}{2}} = 10{\cdot}27$, as was obtained in equation (24).

A plot of A or $A/\beta^{\frac{1}{2}}$ is presented in figure 10. The detailed behaviour of $A/\beta^{\frac{1}{2}}$ in the neighbourhood of $1/\beta = 0$ is examined in Appendix D. If we refer back to figure 3, it may now be recognized that $\Delta f' = \Delta A$ and $\Delta F' = \Delta A/\beta^{\frac{1}{2}}$. A has been evaluated at $\mathbf{R} = 10^5$, but figure 3 could be used to provide the small dependence of A on γ.

Finally γ, or $\lambda = \gamma\beta^{\frac{1}{2}}$, is obtained from equation (26) or (26′) and is plotted in figure 11. At the limit point $1/\beta = 0$, the dependence on $\mathbf{R}$ vanishes.

It will be recalled that the universal shape factor G is defined according to the relation

$$G \equiv \int_0^\infty f'^2 d\eta, \tag{27}$$

or

$$\frac{G}{\beta^{\frac{1}{2}}} = \int_0^\infty F'^2 d\eta. \tag{27'}$$

The values of G are tabulated in table 1 and plotted in figure 12.

When $\beta = \infty$, we have $G/\beta^{\frac{1}{2}} = 5{\cdot}90$ and $\lambda = 0{\cdot}0974$; and since

$$H = [1-\gamma G]^{-1} = [1-\lambda(G/\beta^{\frac{1}{2}})]^{-1},$$

we find that $H = 2{\cdot}35$.

The value of G obtained in the above manner neglects deviations from the logarithmic behaviour in the viscous sublayer. So long as the overlap region is indeed logarithmic, it is a fairly simple matter to obtain a correction for this effect by subtracting out the contribution to equation (27) due to the logarithmic behaviour ($f' = A - (1/\kappa)\ln\eta$) and adding a contribution due to the law of the

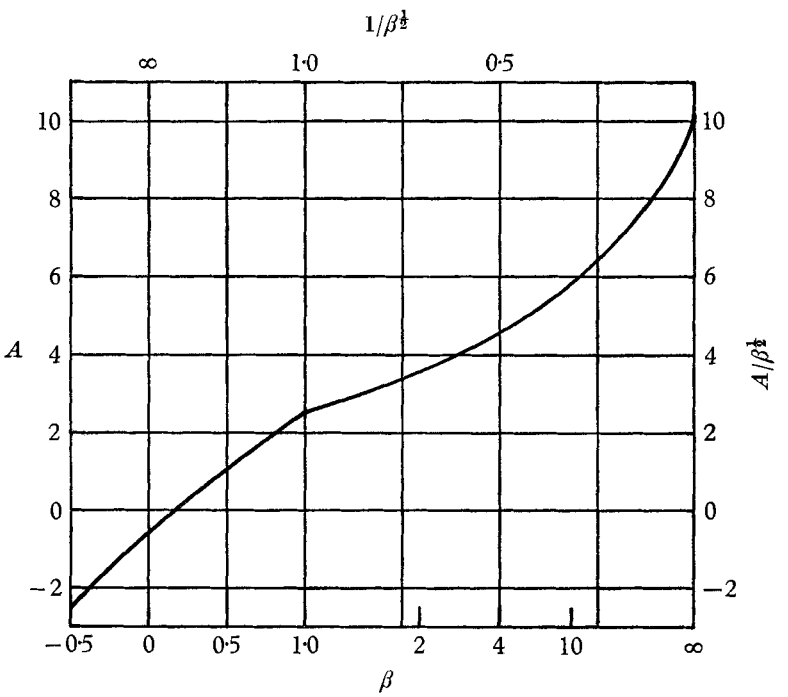

FIGURE 10. The value A in the skin-friction equation.

wall which only becomes logarithmic at some finite value of y. A numerical integration is involved, and without going into detail we note the result that

$$G_{\text{corrected}} = G + \frac{1}{\mathbf{R}}\left(\frac{47}{\gamma} - 580\right). \tag{28}$$

Equation (28) is valid only when the viscous sublayer is not appreciably affected by the pressure gradient. A correction could be established for all β from the results of paper B. In any event the correction is only important for low Reynolds numbers. For example, for $\beta = 0$ and $\mathbf{R} = 10^3$, the uncorrected values of G and H are 6·72 and 1·46 respectively while the corrected values are 7·20 and 1·50; when $\mathbf{R} \geqslant 10^4$, the correction is very small.

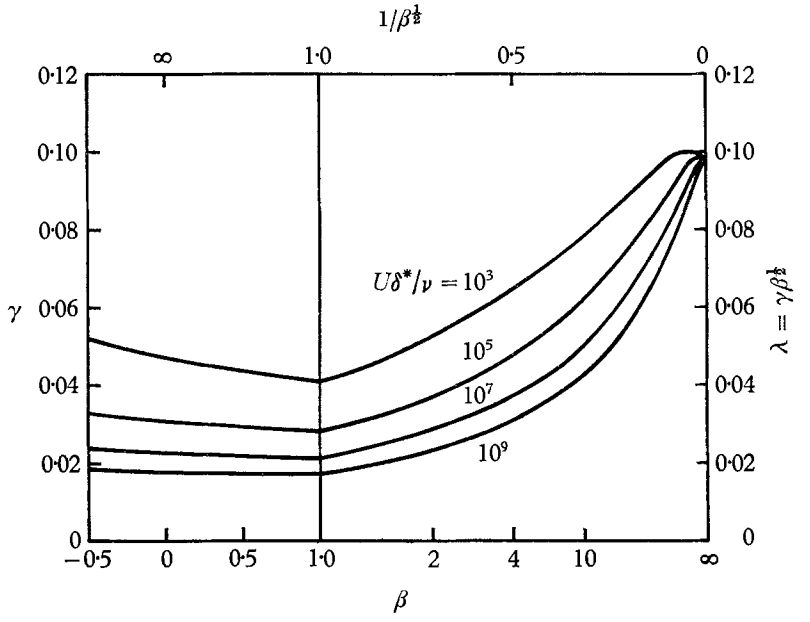

FIGURE 11. The skin-friction coefficient in the form $\gamma = (\frac{1}{2}c_f)^{\frac{1}{2}}$.

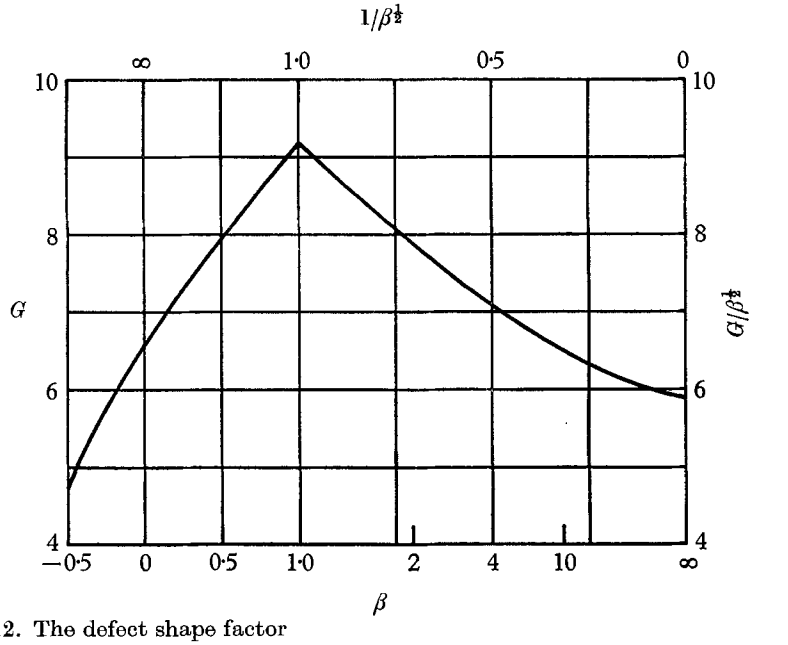

FIGURE 12. The defect shape factor

$$G = \int_0^\infty f'^2\, d\eta.$$

$H = (1-\gamma G)^{-1}$ may be obtained with the aid of figure 11.

Motivation for paper B

The above considerations point to a new problem. For a given β there are small values of **R** where the defect profiles are not logarithmic outside of the viscous sublayer. Our original illustrative example in figure 1*a* has, in fact, been chosen to demonstrate this point. For $\beta = 1$, the match between the wall and the defect layer is poorer for the smaller value of **R**; for larger β, the mismatch is accentuated so that, as $\beta \to \infty$, matching becomes impossible for any value of **R**. This observation challenges the validity of equations (26) and (26′) and it prompted the more detailed inquiry of paper B concerning the flow in the near vicinity of the wall.

9. Variation of $U(x)$ and $\Delta(x)$

It is of interest to examine the particular $U(x)$ and $\Delta(x)$ distributions implied by the equilibrium condition

$$\Delta U'/\gamma U = -\beta, \tag{29}$$

where β is constant. The other governing equation is equation (13*b*), which we will rewrite in the form

$$\frac{\Delta' U}{\Delta U'} = \frac{1}{m} = -1 - \left[H\left(1+\frac{1}{\beta}\right)+1\right]\left[\frac{1+\gamma/\kappa}{1+(\gamma/\kappa)(H-1)}\right], \tag{30}$$

and where we have made use of the identity $H = 1/(1-\gamma G)$. Equation (30) can also be obtained directly from the von Karman momentum-integral equation.

Now, equations (29) and (30) may be rigorously solved together with equation (26) and the values $A(\beta)$ and $G(\beta)$; the latter would account for the small variation of γ and H with x. However, to obtain simple approximate results, we will take $m(x)$ as constant. Equation (30) may then be integrated to give

$$\frac{\Delta}{\Delta_0} = \left(\frac{U}{U_0}\right)^{1/m} \tag{31}$$

where the subscript 0 represents initial values at $x = 0$.

The combination of equation (31) with equation (29) and integration yields

$$\frac{U}{U_0} = \left[1 - \frac{\beta\gamma_0^2}{m}\frac{\tilde{x}}{\delta_0^*}\right]^m, \tag{32}$$

where $\tilde{x} \equiv \int_0 (\gamma/\gamma_0)\,dx$, and also

$$\frac{\Delta}{\Delta_0} = \frac{\gamma_0\delta^*}{\gamma\delta_0^*} = 1 - \frac{\beta\gamma_0^2}{m}\frac{\tilde{x}}{\delta_0^*}. \tag{33}$$

If β is varied so that the right-hand side of equation (30) vanishes, then $m \to \pm\infty$; the right-hand sides of equations (32) and (33) become, in this limit, $\exp[-\beta\gamma_0^2\tilde{x}/\delta_0^*]$ and 1 respectively.

Finally, in the limit $\beta \to \infty$, the combination $\beta\gamma_0^2$ may be replaced by $\lambda^2 = 0{\cdot}0095$ (equation (24)). For this condition we also found that $H = 2{\cdot}35$. Therefore, $m = -[H+2]^{-1} = -0{\cdot}230$ is the unique value of m at this limiting point.

In figure 13 we illustrate equation (32) for the typical value $\mathbf{R}_0 = U_0\delta_0^*/\nu = 10^5$. Note that figure 13 would only be slightly altered by changes in $\mathbf{R}_0$ (or γ_0), except for a rescaling of the abscissa. A nearly universal plot could be constructed by changing the abscissa to $\beta\gamma_0^2\tilde{x}/\delta_0^*$, but then some direct physical feeling would be lost.

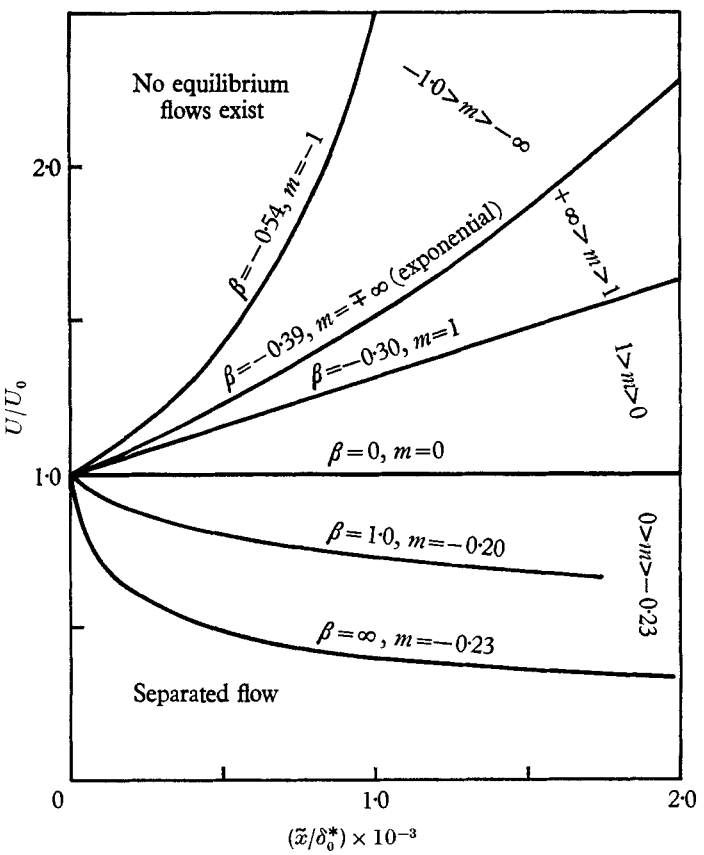

FIGURE 13. Main-stream velocity distributions necessary to produce equilibrium profiles for $R_0 = 10^5$.

Figure 13, therefore, represents a continuous family of solutions with respect to β in the complete range $-0{\cdot}54 \leqslant \beta \leqslant \infty$ (the lower limit corresponding to the condition $m = -1$ at $\mathbf{R}_0 = 10^5$).

Coles's 'law of the wake'

The authors have been asked to compare their findings with the work of Coles (1956), who, from a detailed and thorough examination of experimental data, put forth the following correlation for the defect profile:

$$\frac{U-u}{u_\tau} = -\frac{1}{\kappa}\ln\frac{y}{\delta} + \frac{\pi}{\kappa}\left\{2 - w\left(\frac{y}{\delta}\right)\right\}, \tag{34}$$

where π is a free parameter and the 'wake function' $w(y/\delta)$ is a prescribed function. Besides recognizing the importance of the defect profile, the correlation

represents a synthesis of a great deal of experimental data. In particular, Coles (1956) has shown that the correlation profile does agree with Clauser's data and therefore our calculated curves at least up to $\beta \simeq 10$; and one sees from figure 4 that the case $\pi = 0$ does agree well with the limiting case $\beta = -0{\cdot}5$. However, as $\beta \to \infty$ (and $u_\tau \to 0$ while, presumably, $u_\tau \pi \to$ const.) the correlation does not check with Stratford's data or our calculated result.

In search of a connexion between π and an equilibrium-flow parameter, Coles (1957) has proposed the condition $D = $ const., where, in our present nomenclature, $D-1 \equiv \gamma' U/\gamma U'$ (see equation (13a)). Coles correctly identifies the condition $D = 1$ with the limiting case (which he calls 'pure wall flow'), $m = -1$ or $\beta \simeq -0{\cdot}5$. The prediction is based on an extrapolation of experimental observation, and also on arguments which are presented as deductive arguments; but we do not understand the *a priori* basis of these arguments. However, we now know that D is a second-order parameter which is either close to 1 or has an awkward singularity at $\beta = 0$, and, in general, is not only dependent on β but is also strongly dependent on γ (see equation (13a) and (13b)); it is therefore not a parameter suitable for characterizing equilibrium flows.

By comparing Coles's profile for small η with equation (25a), we find that $2\pi/\kappa = A(\beta) - (\ln \eta_0)/\kappa$, where $\eta_0 \equiv \delta/\Delta$, may be determined from table 1. Thus π may be simply related to β, which, we believe, is the fundamental parameter of equilibrium turbulent boundary layers as originally proposed by Clauser.

10. Conclusions

Equations (9) and (10) together with the empirical constants $\kappa = 0{\cdot}41$ and $K = 0{\cdot}016$ suffice to predict equilibrium turbulent defect profiles in the complete range $-0{\cdot}5 \leqslant \beta \leqslant \infty$ with considerable precision.

Matching the defect profiles with the logarithmic law of the wall (equation (1)) provides a skin-friction equation and brings in a third empirical constant, $\beta = 4{\cdot}9$. Details of the matching procedure are re-examined in paper B.

The three empirical constants are a reflexion of our inherent inability to deal directly with turbulent flow. Nevertheless, it appears that we have attained a rather complete and detailed knowledge of the behaviour of equilibrium turbulent boundary layers.

Appendix A: behaviour of f' for large η

For simplicity we shall discuss the behaviour of equation (21). As indicated in § 5, the discussion of equation (14) involves no new considerations.

For $\beta > -0{\cdot}5$, set

$$f_0' = e^{-x} y(x), \quad x = \frac{1+2\beta}{K}\frac{\eta^2}{2}. \tag{35a, b}$$

Substituting (35a, b) into equation (21), we obtain

$$xy'' + (c-x)y' - ay = 0, \tag{36}$$

where $c = 1/2$ and $a = 1/2(1+2\beta)$. Equation (36) is a confluent hypergeometric

function and, for our purposes, is discussed in a convenient way by Jeffries (1962). Solutions to equation (36) are

$$y_1 = M(a,c;x) = 1+\frac{a}{c}x+\frac{a(a+1)}{c(c+1)}\frac{x^2}{2!}+\ldots, \tag{37}$$

and
$$y_2 = x^{1-c}M(1+a-c,2-c;x). \tag{38}$$

A solution of the form

$$y_3 = \frac{(-c)!}{(a-c)!}y_1+\frac{(c-2)!}{(a-1)!}y_2 \tag{39}$$

is of interest to us since, for large positive x,

$$y_3 \sim x^{-a}\left\{1+O\left(\frac{1}{x}\right)\right\}. \tag{40}$$

Equations (40) and (35a) yield the result quoted in § 5. Any other combination of y_1 and y_2 has a leading term like $e^x x^{a-c}$. This gives the result that $f_0' \sim \eta^{-2\beta/(1+2\beta)}$ or that $f_0 \sim \eta^{1/(1+2\beta)}$. Thus $f_0 \to \infty$ as $\eta \to \infty$ and this solution is rejected.

For $\beta < -0{\cdot}5$, set

$$f_0'(\eta) = y(x); \quad x = -\frac{1+2\beta}{K}\frac{\eta^2}{2}, \tag{41}$$

so that x is positive. We obtain equation (36), where now $c = -\frac{1}{2}$ and $a = -\beta/(1+2\beta)$. For large positive x, all solutions give $y \to \infty$ as $x \to \infty$.

Appendix B: Two-term expansion of equation (14) or (18)

Dealing first with equation (14), we set

$$f = f_0+\gamma f_1+\ldots, \tag{42a}$$

where we will retain only the first and second term in the series. Furthermore,

$$\Phi = \Phi_0+\gamma\Phi_1+\ldots, \tag{42b}$$

$$G = G_0+\gamma G_1+\ldots, \tag{42c}$$

where
$$G_0 \equiv \int_0^\infty f_0'^2\,d\eta, \quad G_1 = 2\int_0^\infty f_0'f_1'\,d\eta,$$

$$\frac{1}{m}+1 = -\left(\frac{1}{\beta}+2\right)-\gamma\left[G_0\left(\frac{1}{\beta}+1\right)+\frac{1}{\kappa}\left(\frac{1}{\beta}+2\right)\right]+\ldots. \tag{42d}$$

Inserting equations (42) into (14) and collecting coefficients of γ^0 and γ^1, we obtain

$$(\Phi_0 f_0'')'+(1+2\beta)\eta f_0''+2\beta f_0' = 0, \tag{43a}$$

$$\begin{aligned}(\Phi_0 f_1'')'+(\Phi_1 f_0'')'+(1+2\beta)\eta f_1'+2\beta f_1' \\ = -(1+\beta)G_0\eta f_0''+(1+2\beta)(f_0 f_0''-f_0'/\kappa-\eta f_0''/\kappa)+\beta f_0'^2,\end{aligned} \tag{43b}$$

whose boundary conditions are

$$\lim_{\eta\to\infty} f_0(\eta) = 1, \tag{44a}$$

$$f_0(0) = 0, \tag{44b}$$

$$\lim_{\eta\to 0}\Phi_0(\eta)f_0''(\eta) = -1, \tag{44c}$$

$$\lim_{\eta\to\infty} f_1(\eta) = 0, \tag{45a}$$

$$f_1(0) = 0, \tag{45b}$$

$$\lim_{\eta\to 0} [\Phi_0(\eta) f_1''(\eta) + \Phi_1 f_0''(\eta)] = 0. \tag{45c}$$

Equations (43a) and (43b) may be integrated once with the help of the boundary conditions to give

$$\Phi_0 f_0'' + (2\beta+1)\eta f_0' - f_0 = -1, \tag{46a}$$

$$\Phi_0 f_1'' + \Phi_1 f_0'' + (2\beta+1)\eta f_1' - f_1 = -(\beta+1)\left[\int_0 f_0'^2\, d\eta + G_0(\eta f_0' - f_0)\right] + (2\beta+1)(f_0' f_0 - \eta f_0'/\kappa), \tag{46b}$$

The remaining boundary conditions are (44a, b) and (45a, b).

Now, corresponding to equation (16) we can write

$$\left.\begin{aligned} \Phi_0 &= Z_0(\eta), \quad \eta \leqslant e, \\ &= K, \quad \eta \geqslant e, \end{aligned}\right\} \tag{47a}$$

and

$$\left.\begin{aligned} \Phi_1 &= Z_1(\eta), \quad \eta < e, \\ &= 0, \quad \eta > e, \end{aligned}\right\} \tag{47b}$$

where

$$Z_0 = \kappa^2\eta^2 |f_0''|, \quad Z_1 = \kappa^2\eta^2 f_1'' \operatorname{sgn}(f_0''),$$

and e is the first root of the equation $Z_0(e) = K$. Equation (47b) requires some explanation. It derives from an expansion of Φ in the form

$$\Phi(Z_0 + \gamma Z_1) = \Phi(Z_0) + \Phi'(Z_0)\gamma Z_1 + \ldots,$$

so that $\Phi_1 = \Phi'(Z_0) Z_1$. But $\Phi'(Z_0) = 1$ for $\eta < e$ and $\Phi'(Z_0) = 0$ for $\eta > e$, thereby giving equation (47b).

Equation (18) may be treated in a similar manner, or we may directly substitute $f_0(\eta) = F_0(\xi), f_1(\eta) = \beta^{\frac{1}{2}} F_1(\xi)$ and $\eta = \xi/\beta^{\frac{1}{2}}$ into equations (43a, b) or (46a, b).

Appendix C: notes on the numerical computations

Solutions from equations (46a, b)

(a) The equations were solved iteratively. An initial guess, according to equation (10′), was made for Φ_0 when $\eta \leqslant e$. Equation (46a) was then treated as a linear equation. The combination $\Phi_0 f_1'' + \Phi_1 f_0''$ in equation (46b) is equivalent to $2\Phi_0 f_0''$ when $\eta < e$, but $\Phi_0 f_1''$ when $\eta > e$, and equation (46b) is therefore linear.

(b) At each iteration, a particular solution (for f_0 it is 1) and solutions to the homogeneous equations were obtained using a third-degree Runga–Kutta method (Hildebrand 1949). The solutions were combined linearly to satisfy the boundary conditions.

(c) At each iteration, a new estimate of Φ_0 (when $\eta < e$) was made by combining equation (46a) with (47a) and taking the square root. This gives $\Phi_0 = \kappa\eta[1 + (1+2\beta)\eta f_0' - f_0]^{\frac{1}{2}}$ and shows the close resemblance to equation (10′) for small β and η.

(d) The logarithmic singularity at $\eta = 0$ may be removed by setting $f_0 = 1 + c_1 u_1 + c_2(u_1 \ln\eta + u_2)$; u_1 and u_2 are then regular at $\eta = 0$. However,

solutions obtained by this procedure and from the equation for F_0, where we set $F_0 = 1 + c_1 u_1 + c_2 u_2$ (the inner boundary conditions were fixed at $\eta = 0{\cdot}0001$ so that $F_0(0{\cdot}0001) = 0{\cdot}0001 F_0'(0{\cdot}0001)$), agreed in the second decimal place when $\beta = 1/\beta = 1$.

(*e*) The outer boundary condition was set at a finite $\eta = \eta_2$, so that $f_0(\eta_2) = 1$. η_2 was chosen large enough so that $1 - f_0(\eta_1) \leqslant 10^{-3}$, where $\eta_2 - \eta_1 \geqslant 0{\cdot}2$. An independent check on the accuracy was that $f_0'(\eta) \to 0{\cdot}000$ as $\eta \to \eta_2$.

(*f*) Only three of four iterations were necessary to converge to the third decimal place. This was assisted by using an initial guess, Φ_0, for each calculation in β, corresponding to the Φ_0 determined by the previous calculations in β.

(*g*) By varying the integrating increment, it was determined that all decimal places published are (numerically) significant.

Solutions directly from equation (14)

Our previous experience indicates a method of solution directly from equation (14) or equation (19) which is strongly convergent. We first integrate equation (14) once to give

$$\Phi f'' - \beta\left(\frac{1}{m}+1\right)\left[\eta f' - \left(\frac{1}{1+\gamma/\kappa}\right) f - \gamma\left(\frac{1}{1+\gamma/\kappa}\right) f f' + \gamma\left(\frac{1-\gamma/\kappa}{1+\gamma/\kappa}\right)\int_0 f'^2\, d\eta\right] + \beta\left(2f - \gamma\int_0 f'^2\, d\eta\right) = -1, \quad (14')$$

or for equation (18) we have

$$\Phi F'' - \left(\frac{1}{m}+1\right)\left[\xi F' - \left(\frac{1}{1+\lambda/\kappa\beta^{\frac{1}{2}}}\right) F - \lambda\left(\frac{1}{1+\lambda/\kappa\beta^{\frac{1}{2}}}\right) F F' + \lambda\left(\frac{1-\lambda/\kappa\beta^{\frac{1}{2}}}{1+\lambda/\kappa\beta^{\frac{1}{2}}}\right) \times \int_0 F'^2\, d\xi\right] + 2F - \lambda\int_0 F'^2\, d\xi = -\frac{1}{\beta}. \quad (18')$$

Arrange the result in two parts; the first part is identical in form with equation (46*a*) and the second part is the remainder R. The equation is solved in the same manner as f_0 or F_0 above but in obtaining a 'particular solution' $R(\eta)$ or $R(\xi)$ is included and is determined from the previous iteration. Initially $R = 0$. (If $R = 0$ were inserted at every iteration we would obtain $f = f_0$ or $F = F_0$, which is a fair approximation to the exact solution.)

Appendix D: the behaviour of $A/\beta^{\frac{1}{2}}$ in the neighbourhood of $1/\beta = 0$

In the neighbourhood of $1/\beta = 0$, the left-hand side of equation (18′) in Appendix C contains parameters which are virtually independent of β.

Now, for very small ξ, equation (18′) may be written

$$\Phi F'' = -1/\beta, \quad (48)$$

and since $\Phi = \kappa^2\xi^2 |F''|$ we can obtain

$$F' = \frac{A}{\beta^{\frac{1}{2}}} - \frac{1}{\kappa\beta^{\frac{1}{2}}} \ln\frac{\xi}{\beta^{\frac{1}{2}}}, \quad (49)$$

where $A/\beta^{\frac{1}{2}} + (1/\kappa\beta^{\frac{1}{2}}) \ln \beta^{\frac{1}{2}}$ is the constant of integration. Knowing the behaviour of F' (equation (49)), one can assess the terms in equation (18′), show that

$$\int_0 F'^2 d\xi \simeq FF' \simeq \xi F'^2$$

and find that the next-order approximation for $\Phi F''$ is

$$\Phi F'' = -(H+1)\xi F' + 2\lambda \xi F'^2 - (1/\beta). \tag{50}$$

For very small ξ, $1/\beta$ is larger than the other terms on the right-hand side of equation (50). At some $\xi = a$, these other terms become comparable with $1/\beta$, so that

$$\frac{aF'(a)\,[H+1-2\lambda F'(a)]}{(1/\beta)} = b, \tag{51}$$

where $b = O(1)$.

Now, as a rough approximation, we presume that: (*a*) when $\xi < a$, equation (49) is valid; (*b*) when $\xi > a$, equation (18′) with $1/\beta$ set equal to 0 is valid.

Statement (*b*), together with the boundary conditions

$$F'(\infty) = 0 \quad \text{and} \quad F(a) \simeq F(0) = 0,$$

merely asserts that $F'(a)$ can only vary a small amount with respect to β as $1/\beta \to 0$; in fact, as $1/\beta \to 0$, $a \to 0$ and $F'(a) \to 10{\cdot}27$, so that combining equation (51) and (49) yields

$$\frac{A}{\beta^{\frac{1}{2}}} = 10{\cdot}27 + \frac{1}{\kappa\beta^{\frac{1}{2}}} \ln\left(\frac{b}{13{\cdot}8\beta^{\frac{3}{2}}}\right). \tag{52}$$

It will be noticed that our final result is only weakly dependent on b as $1/\beta \to 0$. If we, finally, set $b = 1{\cdot}4$ we obtain a result which nicely fairs in with the calculated points in the range $0 \leqslant 1/\beta \leqslant 0{\cdot}1$.

The work was carried out under the Bureau of Ships Fundamental Hydromechanics Research Program, SR 009 01 01, administered by the David Taylor Model Basin; contract Nonr-1858(38).

REFERENCES

Clauser, F. 1954 Turbulent boundary layers in adverse pressure gradients. *J. Aero. Sci.* **21**, 91–108.

Clauser, F. 1956 The turbulent boundary layer. *Adv. Appl. Mech.* **4**, 1–51.

Coles, D. 1956 The law of the wake in the turbulent boundary layer. *J. Fluid Mech.* **1**, 191–226.

Coles, D. 1957 Remarks on the equilibrium turbulent boundary layer. *J. Aero. Sci.* **24**, 495–506.

Gibson, D. M. & Mellor, G. L. 1962 Incompressible boundary layers in adverse pressure gradients. *Mech. Eng. Rep., FLD* 5, *Princeton University.*

Hartree, D. R. 1937 On an equation occurring in Falkner and Skan's approximate treatment of the equations of the boundary layer. *Proc. Camb. Phil. Soc.* **33**, 223–39.

Hildebrand, F. B. 1949 *Advanced Calculus for Engineers.* New York: Prentice-Hall Inc.

Jeffries, H. 1962 *Asymptotic Approximation.* Oxford University Press.

Ludwig, H. & Tillman, W. 1950 Investigation of the wall shearing stress in turbulent boundary layers. *NACA TM* no. 1285.

Mellor, G. L. 1966 The effect of pressure gradients on the flow near a smooth wall. *J. Fluid Mech.*, **24**, 255.

MILLIKAN, C. B. A. 1938 A critical discussion of turbulent flows in channels and circular tubes. *Proc. Fifth Int. Congress Appl. Mech.* pp. 386–92.

ROTTA, J. 1950 Über die Theorie der tubulenten Grenzschichten, *Mitt. Max-Planck-Inst., Gottingen, No.* 1; translated as (1953): On the theory of the turbulent boundary layer. *Nat. Adv. Comm. Aero., Wash., Tech. Mem.* no. 1344.

STRATFORD, B. S. 1959*a* The prediction of separation of the turbulent boundary layer. *J. Fluid Mech.* **5**, 1–16.

STRATFORD, B. S. 1959*b* An experimental flow with zero skin friction throughout its region of pressure rise. *J. Fluid Mech.* **5**, 17–35.

TOWNSEND, A. A. 1956 The properties of equilibrium boundary layers. *J. Fluid Mech.* **1**, 561–73.

TOWNSEND, A. A. 1960 The development of turbulent boundary layers with negligible wall stress. *J. Fluid Mech*, **8**, 143–55.

TOWNSEND, A. A. 1961 Equilibrium layers and wall turbulence. *J. Fluid Mech.* **11**, 97–120.